

**MOLECULAR DOCKING AND MOLECULAR
DYNAMICS OF 3-O-OCTANOYL CATECHIN
INTERACTIONS AGAINST ALDOSE
REDUCTASE**

SHIKIN FAEZAH BINTI SOIB

UNIVERSITI SAINS MALAYSIA

2019

**MOLECULAR DOCKING AND MOLECULAR
DYNAMICS OF 3-O-OCTANOYL CATECHIN
INTERACTIONS AGAINST ALDOSE
REDUCTASE**

by

SHIKIN FAEZAH BINTI SOIB

Thesis submitted in fulfilment of the requirements

for the degree of

Master of Sciences

August 2019

ACKNOWLEDGEMENT

Alhamdulillah. First and foremost, I would like to express my deepest gratitude to my beloved supervisor, Prof. Dr. Rohana binti Adnan for her tremendous guidance, knowledge and support. Her constructive comments and suggestions as well as her positive words motivate me to work harder and to never quit to complete this study. My appreciation also goes to my co-supervisor, Dr. Hasni bin Arsad for his support and knowledge. I would like to sincerely thank all my group members and friends, Amneh, Fitrah, Mimi, Azia, Farah, Mira, Solehah, Kak Erma, Najm, Irfan, Saifullah, Kak Nazihah and Jaga for their help, moral support and for always being there cheering me up through the good and the bad times.

My special thanks go to my beloved and lovely parents, Mak and Ayah, for their constant encouragement, support and for always believing in me. Next, I owe my special gratitude to my siblings for their non-stop support and motivation for me to continue the study.

I also wish to thank all the staff of School of Chemical Sciences, USM for their technical support and help throughout my study. Finally, I owe my gratitude to our university, USM for the financial support through the Fellowship Scheme under the Institute of Postgraduate Studies and also through the FRGS grant number 1001/PKIMIA/6711558.

TABLE OF CONTENTS

ACKNOWLEDGEMENT	ii
TABLE OF CONTENTS	iii
LIST OF TABLES	vi
LIST OF FIGURES	vii
LIST OF ABBREVIATIONS	x
LIST OF SYMBOLS	xii
ABSTRAK	xiii
ABSTRACT	xv
CHAPTER 1 - INTRODUCTION	1
1.1 Introduction	1
1.2 Problem Statement	3
1.3 Objectives	4
1.4 Scope of This Study	4
CHAPTER 2 – LITERATURE REVIEW	5
2.1 Diabetes and Its Complications	5
2.2 Aldose Reductase, Polyol Pathway and Its Inhibitors	7
2.2.1 Polyol Pathway Mechanism and Oxidative Stress	7
2.2.2 Structure of Aldose Reductase	10
2.2.3 Development of Aldose Reductase Inhibitors	12
2.3 Flavonoids and Catechin	14

2.4	Molecular Modelling	18
2.4.1	Molecular Docking	18
2.4.1(a)	Scoring Function	25
2.4.1(b)	Search Algorithm	26
2.4.2	Molecular Dynamics	26
CHAPTER 3 - METHODOLOGY		28
3.1	Technical Details	28
3.2	Protein Preparation	28
3.3	Ligand Preparation	29
3.4	Molecular Docking	31
3.5	Molecular Dynamics (MD) Simulation	31
3.5.1	Initialization	32
3.5.2	Equilibration	32
3.5.3	Production Run	33
3.5.4	Trajectory Analysis	33
3.6	Molecular Mechanics Poisson-Boltzmann Surface Area (MM-PBSA) Free Energy Calculation Analysis	35
CHAPTER 4 – RESULTS AND DISCUSSION		38
4.1	ADME Properties of Catechin Derivatives	38
4.2	Molecular Docking	39
4.2.1	The Structure of Aldose Reductase	39
4.2.2	Validation of Molecular Docking Procedure	40
4.2.3	The Binding Free Energy and the Interactions of AR/NADP+ Complex with Catechin Derivatives via Molecular Docking.	41
4.3	Molecular Dynamics Simulation	51
4.3.1	Structural Stability Analysis	51

4.3.1(a) Root Mean Square Deviation	51
4.3.1(b) Radius of Gyration	53
4.3.1(c) Secondary Structure Analysis	54
4.3.2 Flexibility and Conformational Change Analysis	55
4.3.3 Hydrogen Bond Analysis	57
4.3.3(a) Number of Hydrogen Bond Formation Throughout the Simulations	57
4.3.3(b) The Occupancy of Hydrogen Bonds Throughout the 100 ns Simulations	59
4.4 MM-PBSA Analysis	62
CHAPTER 5 - CONCLUSIONS	67
5.1 Conclusions	67
5.2 Recommendations for Future Work	68
REFERENCES	69
APPENDICES	

LIST OF TABLES

		Page
Table 2.1	The chronic complications of diabetes (Williams et al., 2002).	6
Table 2.2	Classes of flavonoids and their examples.	14
Table 2.3	Summary of the studies reported on ARIs via molecular docking and molecular dynamics simulation methods used (if any) over the last 10 years.	20
Table 4.1	The summaries of the properties of the catechin compounds according to the Lipinski's Rule of Five determined by SwissADME online tool.	38
Table 4.2	The interactions and binding energies of AR/NADP+ complex with catechin derivatives from molecular docking studies (D = donor, A = acceptor, AR = aldose reductase and L = ligand).	42
Table 4.3	The comparison of the calculated average RMSD values for different complexes.	51
Table 4.4	The percentage of secondary structure of AR in each complex during the last 10 ns simulation time.	54
Table 4.5	The list of donor and acceptor atoms of the intermolecular hydrogen bond formations for all complexes.	60
Table 4.6	The total binding energies and its components for AR/NADP+ complex with quercetin and ligands 2 .	63

LIST OF FIGURES

		Page
Figure 2.1	Polyol pathway (Aslan & Beydemir, 2017).	8
Figure 2.2	Possible pathways for glucose (Gallagher et al., 2016).	9
Figure 2.3	Crystal structure of aldose reductase with cofactor NADP ⁺ (green) and the bound ligand IDD 594 (blue) from Protein Data Bank with PDB ID of 1US0 (Howard et al., 2004). The α -helices are highlighted in orange while the β -sheets are highlighted in purple colour. The coils are coloured in grey. The graphic is prepared using Chimera software.	10
Figure 2.4	The reduction of NADP ⁺ (the oxidised form of NADPH) to NADPH.	11
Figure 2.5	The binding pocket of AR in order of increasing degree of flexibility (blue < purple < orange < red) (Gopinath et al., 2016; Sottriffer et al., 2004).	12
Figure 2.6	Chemical structures of known ARIs.	13
Figure 2.7	Basic structure of flavonoid.	14
Figure 2.8	Schematic illustration of docking a small molecule or ligand (green) to a protein or macromolecule (black) to produce a stable protein/ligand complex.	19
Figure 3.1	Catechin derivatives used in this study.	30
Figure 3.2	Criteria for hydrogen bond formation (where D = hydrogen donor, A = hydrogen acceptor and H = hydrogen atom).	35
Figure 3.3	The flow chart of the steps and methods used in this study.	37
Figure 4.1	The structure of [2-(4-bromo-2-fluorobenzylthiocarbamoyl)-5-fluoro-phenoxy] acetic acid or IDD 594.	40

Figure 4.2	Superimposed view of re-docked pose (gray) of IDD594 with the original co-crystallised ligand (black) with RMSD value of 5.36 nm. The structures are prepared using Chimera software.	40
Figure 4.3	2D representation of crystal structure IDD594 at AR binding site for PDB ID 1US0 (black = carbon, red = oxygen, blue = nitrogen, yellow = sulphur, dashed green line = hydrogen bond and red region = hydrophobic interaction). This graphic is prepared using Ligplot.	45
Figure 4.4	The chemical structure of quercetin.	46
Figure 4.5	Mechanism proposed by Dréanic et al. (2017) regarding AR reaction where TS is the transition state.	48
Figure 4.6	The overlay of ligand 2 (pink) with quercetin (blue) and the hydrogen bonding interactions of ligand 2 with AR. This graphic is presented using PyMol software.	49
Figure 4.7	2D representation of the interactions of AR with (a) quercetin and (b) ligand 2 (black = carbon, red = oxygen, blue = nitrogen, yellow = sulphur, dashed green line = hydrogen bond and red region = hydrophobic interaction). This figure is prepared using Ligplot software.	50
Figure 4.8	Root mean square deviations of the backbone of free AR/NADP ⁺ (black), AR/NADP ⁺ /quercetin complex (red) and AR/NADP ⁺ /ligand 2 complex (green) with function of time.	52
Figure 4.9	Radius of gyration of the backbone of free AR/NADP ⁺ (black), AR/NADP ⁺ /quercetin complex (red) and AR/NADP ⁺ /ligand 2 complex (green) as a function of time.	53
Figure 4.10	Root mean square fluctuations of the amino acid residues of AR/NADP ⁺ complex (black), AR/NADP ⁺ /quercetin complex (red) and AR/NADP ⁺ /ligand 2 complex (green).	56

Figure 4.11	The conformations of free AR/NADP ⁺ during (a) 0 ns and (b) 100 ns. Number 1-4 represent the regions labelled in the graphs of RMSF (Figure 4.10). This structure is prepared using Chimera software.	57
Figure 4.12	The number of hydrogen bonds formed between quercetin and AR/NADP ⁺ complex throughout the simulation time.	58
Figure 4.13	The number of hydrogen bonds formed between ligand 2 and AR/NADP ⁺ complex throughout the simulation time.	58
Figure 4.14	The percentage occupancy of intermolecular hydrogen bond formations of AR/NADP ⁺ complex with (a) quercetin, (b) ligand 2 , which formed with more than 1 % occupancy throughout the simulation time arranged in the order of highest to lowest percentage occupancy for each amino acid.	61
Figure 4.15	The average energy contributed by each residue for the last 10 ns simulation time (a) and the interaction of quercetin with AR at 100 ns (b). The figure is prepared using PyMol software.	65
Figure 4.16	The average energy contributed by each residue for the last 10 ns simulation time (a) and the interaction of ligand 2 with AR at 100 ns (b). The figure is prepared using PyMol software.	66

LIST OF ABBREVIATIONS

IDD 594	[2-(4-bromo-2-fluorobenzylthiocarbamoyl)-5-fluoro-phenoxy] acetic acid
AGEs	Advanced glycation end products
Ala	Alanine
AR	Aldose reductase
ARIs	Aldose reductase inhibitors
CVD	Cerebral artery disease
NPT	Constant number of molecules, pressure and temperature
NVT	Constant number of molecules, volume and temperature
CAD	Coronary artery disease
Cys	Cysteine
DM	Diabetes Mellitus
GA	Genetic algorithm
Glu	Glutamic acid
Gln	Glutamine
GSH	Glutathione
GROMACS	Groningen Machine for Chemical Simulation
His	Histidine
PDB ID	Identification of entries in Protein Data Bank
LGA	Lamarckian genetic algorithm
Leu	Leucine
Lys	Lysine
MD	Molecular dynamics
MM-GBSA	Molecular mechanics generalised Born surface area

MM-PBSA	Molecular mechanics Poisson-Boltzmann surface area
NCBI	National Center for Biotechnology Information
NADH	Nicotinamide adenine dinucleotide
NADPH	Nicotinamide adenine dinucleotide phosphate
NAD ⁺	Oxidised form of nicotinamide adenine dinucleotide
NADP ⁺	Oxidised form of nicotinamide adenine dinucleotide phosphate
PM3	Parameterized model number 3
PVD	Peripheral vascular disease
Phe	Phenylalanine
Pro	Proline
PDB	Protein Data Bank
R _g	Radius of gyration
ROS	Reactive oxidative species
RMSD	Root-mean-square deviation
RMSF	Root-mean-square fluctuation
SASA	Solvent accessible surface area
SCF	Self-consistent field
SDH	Sorbitol dehydrogenase
Thr	Threonine
TIP3P	Transferable intermolecular potential with 3 points
Trp	Tryptophan
Tyr	Tyrosine
Val	Valine
VMD	Visual Molecular Dynamics

LIST OF SYMBOLS

a_i	Acceleration of particle i
B_i	B-factor
F_i	Force exerted on particle i
fs	Femtosecond
$G_{complex}$	Free energy of complex
G_{ligand}	Free energy of ligand
$G_{protein}$	Free energy of protein
K	Kelvin
Log P	Octanol-water partition coefficient
M	Total protein mass
m_i	Mass of particle i
nm	Nanometre
ns	Nanosecond
ps	Picosecond
R^\bullet	Free radical
r_i	Position of particle i
U	Potential energy of the system
ΔE_{bonded}	Energy of bonded interactions
ΔE_{elec}	Electrostatic energy
ΔE_{MM}	Average molecular mechanics potential energy in vacuum
$\Delta E_{nonbonded}$	Energy of non-bonded interactions
ΔE_{vdw}	Van der Waals energy
$\Delta G_{binding}$	Binding free energy
ΔG_{sol}	Solvation free energy

**PENDOKKAN MOLEKUL DAN DINAMIK MOLEKUL INTERAKSI
3-O-OKTANOILKATECIN TERHADAP ALDOSA REDUKTASE**

ABSTRAK

Kajian ini dijalankan untuk mencari perencat aldosa reduktase (AR) berpotensi dalam kalangan terbitan katecin terpilih menggunakan kaedah pengkomputeran. Pendokkan molekul, simulasi dinamik molekul dan pengiraan tenaga bebas mekanik molekul luas permukaan Poisson-Boltzmann (MM-PBSA) telah dilakukan untuk mengkaji interaksi AR dengan terbitan-terbitan katecin. Sejumlah 14 ligan terbitan katecin telah diutarakan untuk pendokkan molekul. Keputusan pendokkan molekul menunjukkan bahawa ligan **2** (3-*o*-oktanilkatecin) mempunyai interaksi terbaik dan tenaga pengikat terendah dengan AR. Satu simulasi dinamik molekul (MD) 100 ns telah dijalankan untuk kedua-dua kompleks AR/NADP⁺/kuersetin (standard) dan AR/NADP⁺/ligan **2**. Keputusan analisis MD telah mengesahkan kestabilan kompleks AR/NADP⁺/ligan **2** berdasarkan keputusan sisihan punca-min-kuasa dua (RMSD), jejari legaran (R_g) dan analisis struktur sekunder. Keputusan pergolakan punca-min-kuasa dua (RMSF) menyatakan bahawa tiada perubahan besar dalam struktur dan konformasi protein apabila ligan **2** mengikat. Analisis ikatan hidrogen menunjukkan bahawa ligan **2** memiliki bilangan dan kependudukan pembentukan ikatan hidrogen antara molekul yang tinggi dengan Trp111 (43.2 %), Glu120 (24.3 %), His110 (24.2 %), Gln49 (8.5 %) dan Val47 (2.0 %) sepanjang simulasi berbanding dengan kuersetin. Pengiraan tenaga pengikatan bebas MM-PBSA mendedahkan jumlah tenaga pengikat yang lebih rendah untuk ligan **2** (-127.62 ± 10.82 kJ/mol) berbanding kuersetin (-50.10 ± 9.74 kJ/mol). Keputusan kajian ini juga menunjukkan bahawa interaksi AR dengan ligan **2** adalah kebanyakannya dengan asid amino tidak

polar dan hidrofobik seperti Trp20, Trp111, Phe122 and Leu300. Interaksi ini juga menunjukkan bahawa ligan **2** mengikat pada tapak aktif AR. Keputusan pengkomputeran telah menyimpulkan bahawa ligan **2** atau 3-*o*-oktanoilkatecin mempunyai potensi untuk merencat AR.

**MOLECULAR DOCKING AND MOLECULAR DYNAMICS OF
3-O-OCTANOYLCATECHIN INTERACTIONS AGAINST ALDOSE
REDUCTASE**

ABSTRACT

This study was conducted to search for potential aldose reductase (AR) inhibitors among the chosen catechin derivatives using computational methods. Molecular docking, molecular dynamics (MD) simulation and molecular mechanics Poisson-Boltzmann surface area (MM-PBSA) free energy calculation were performed to investigate the interactions of AR with the catechin derivatives. A total of 14 ligands of catechin derivatives were submitted for molecular docking. Molecular docking results revealed ligand **2** (3-*o*-octanoylcatechin) has the best interactions and lowest binding energy with AR. A 100 ns molecular dynamics (MD) simulation was conducted for both AR/NADP⁺/quercetin (standard) and AR/NADP⁺/ligand **2**. The results of MD analysis confirmed the stability of the AR/NADP⁺/ligand **2** complex based on the results of root-mean-square deviation (RMSD), radius of gyration (R_g) and secondary structure analysis. The root-mean-square fluctuations (RMSF) results indicated that there are no major changes in the structure and conformation of the protein upon the binding of ligand **2**. The hydrogen bond analysis showed that ligand **2** has a high number and occupancy of intermolecular hydrogen bond formation with Trp111 (43.2 %), Glu120 (24.3 %), His110 (24.2 %), Gln49 (8.5 %) and Val47 (2.0 %) throughout the simulation compared with quercetin. The MM-PBSA free energy calculation showed lower total binding energy of ligand **2** (-127.62 ± 10.82 kJ/mol) compared with quercetin (-50.10 ± 9.74 kJ/mol). The results also showed that the interactions of AR with ligand **2** are

mostly with non-polar and hydrophobic amino acids such as Trp20, Trp111, Phe122 and Leu300. This interactions also showed that ligand **2** binds at the active site of AR. The computational results has concluded that ligand **2** or 3-*o*-octanoylcatechin has the potential to inhibit AR.

CHAPTER 1

INTRODUCTION

1.1 Introduction

Diabetes mellitus (DM) is a major health issue that has threatened 415 million people in the world in 2015 and it is expected to rise to 642 million people in 2040 (International Diabetes Federation, 2015). It is a metabolic disorder that occurs due to high blood sugar level in the body (hyperglycaemia), mainly due to the insufficient production of insulin or the insulin produced cannot be used properly by the body or both (Ullah et al., 2016). Diabetes can be divided into three main types, type I, type II and gestational diabetes (American Diabetes Association, 2014).

Type I diabetes happens when the immune system attacks the cells that produce insulin in the pancreas called beta cells, destroying or damaging the cells, leading to little to no insulin production. It usually starts in patients at age younger than 30 (van Belle et al., 2011). Meanwhile, patients with type II diabetes make their own insulin, but their body did not respond well to insulin or insulin insensitive. This will lead to increasing production of insulin that will eventually cause β -cells dysfunction (Kahn et al., 2014). This condition is also called as insulin resistant. Type II diabetes is usually related to poor lifestyles such as the cut down of physical activities and bad eating habits (Zhao et al., 2015). Lastly, gestational diabetes occurs only in pregnant women (American Diabetes Association, 2014).

There are a lot of complications related to diabetes patients. Some examples of the complications are nephropathy (Dunlop, 2000), neuropathy (Veves, 2007; Witzel et al., 2015), cardiovascular disease (Hu et al., 2014), cataract (Patel et al.,

2012c), and retinopathy (Lorenzi, 2007). The proposed cause for these diabetes-induced complications is related to increasing oxidative stress in the body (Niedowicz & Daleke, 2005).

Besides diabetes, oxidative stress also contributes to other pathological conditions and diseases such as cancer, neurological disorders (Parkinson's disease, Alzheimer's disease and Huntington's disease), arteriosclerosis, hypertension, stroke and asthma (Birben et al., 2012; Rahman et al., 2012). Oxidative stress is a condition where the production of free radicals and active intermediates in a system is greater than the system's ability to neutralize and eradicate them (Rahman et al., 2012). In diabetic patients, the generation of free radicals occur through several pathways including increased glycolysis, intercellular activation of polyol pathway, protein kinase C dependent activation of NAD(P)H oxidase, increased hexosamine pathway flux and increased intracellular formation of advanced glycation end products (AGEs) (Chikezie et al., 2015).

The main focus of this study is on the polyol pathway which consists of two enzymatic reactions. Firstly, the conversion of glucose to sorbitol with nicotinamide adenine dinucleotide phosphate (NADPH) as cofactor by enzyme aldose reductase (AR) and then the conversion of sorbitol to fructose using sorbitol dehydrogenase (SDH) with nicotinamide adenine dinucleotide (NAD⁺) as cofactor (Chung et al., 2003). Glucose is usually converted to energy but a hyperglycaemic patient have excess glucose that will increase the rate of polyol pathway and this will eventually cause the oxidative stress in the body (Aslan & Beydemir, 2017). The first reaction is the rate-limiting step in the polyol pathway making it crucial and AR as the target protein for researchers to find the inhibitor (Sangshetti et al., 2014).

In this study, the inhibitors for AR were investigated between a class of flavonoid namely the catechin derivatives. Flavonoids are polyphenolic compounds found mainly in plants (Kumar & Pandey, 2013). Some flavonoids such as quercetin, quercitrin, and luteolin are known to be AR inhibitors (Grewal et al., 2016).

Nowadays, computational method has been broadly used to understand and predict the properties, interactions and behaviour of a system. Molecular docking, structure-based virtual screening and molecular dynamics (MD) simulation are among the most frequently used in drug design strategies due to their wide range of applications (Ferreira et al., 2015). The computational methods used to find new aldose reductase inhibitors (ARIs) were pharmacophore (Chadha & Silakari, 2017), molecular docking (Kondhare et al., 2017), and virtual screening (Wang et al., 2013), while MD simulation was used to understand the behaviour of AR (Rechlin et al., 2017).

1.2 Problem Statement

Extensive research on aldose reductase for these past years has led to the discovery of many AR inhibitors. However, a lot of them did not pass the clinical trials due to their low efficacy, bioavailability and adverse side effects. A more natural resources was sought out by researcher in order to reduce the toxicity and increase the viability. Compounds extracted from plants were tested against AR to find potent AR inhibitors. This research is done to find possible AR inhibitors from chosen catechin derivatives through computational methods. AR is a flexible enzyme and the substrate bind to the active site has different conformations depending on the type of the compound (Sotriffer et al., 2004). Thus, using computational methods such as molecular docking and molecular dynamics simulation, the interaction between AR and its inhibitors can be studied closely at molecular level.

1.3 Objectives

The objectives of this research are:

1. To investigate possible aldose reductase inhibitors from a group of catechin derivatives and their binding mode using molecular docking method.
2. To study more detailed interactions between aldose reductase and catechin derivatives and the stability of the complexes using molecular dynamics simulations.

1.4 Scope of This Study

This study is focused on the interactions of 14 catechin derivatives with aldose reductase, an enzyme responsible for the diabetic complications in humans. High blood glucose level in the body of diabetic patients will increase the rate of reactions of the polyol pathway since the reactant for the pathway is glucose. This will lead to increasing oxidative stress, a condition where the formation of free radicals exceeds the antioxidants activity, which will lead to diabetic complications. The search for aldose reductase inhibitors is still in progress due to the structure of the AR binding site that can fit many types of ligands. Instead of researching for new drugs, it will be more efficient in finding the possible AR inhibitors from the already available natural products. Catechins are mainly found in tea which is a widely known and most consumed beverage in the world (Bhattacharjee, 2015; Kumar & Pandey, 2013). Studies have shown that catechins can inhibit AR but with lower inhibition activities among the flavonoids (Matsuda et al., 2002; Murata et al., 1994). Thus, catechin derivatives were chosen to be tested against AR in order to investigate their potential as AR inhibitors.

CHAPTER 2

LITERATURE REVIEW

2.1 Diabetes and Its Complications

Diabetes mellitus (DM) is probably one of the oldest diseases known to man. It was first characterised in an Egyptian manuscript dated 3000 years ago (Lakhtakia, 2013; Olokoba et al., 2012). DM has become one of the major health concerns in 21st century and in 2015 alone, one out of 11 adults has diabetes according to International Diabetes Federation (2015), with Asian countries representing more than 60 % of the world's diabetic population (Ramachandran et al., 2012). There are several factors that increase the prevalence of DM. For example, type I diabetes occurs mainly due to β -cell destruction, while type II diabetes occurs mainly due to insulin resistance. DM is also associated with lifestyles and genetics (Patel et al., 2012b).

DM is characterized by the elevation of blood glucose level in the body (hyperglycaemia). Chronic hyperglycaemia has various macrovascular and microvascular complications which are summarized in Table 2.1. Diabetes and its complications are the major causes of death in most countries. According to International Diabetes Federation (2015), patients with diabetes are at higher chance of having life-threatening health complications than those without it.

Table 2.1 The chronic complications of diabetes (Williams et al., 2002).

System affected	Disease
Eyes	Retinopathy, Glaucoma Cataracts Blindness
Blood vessels	Coronary artery disease (CAD) Cerebral vascular disease (CVD) Peripheral vascular disease (PVD) Hypertension
Kidneys	Renal insufficiency Kidney failure
Nerves	Neuropathies Autonomic neuropathy
Skin, Muscle, Bone	Advanced infections Cellulitis Gangrene Amputation

Researchers have investigated ways to prevent and reduce the effect of diabetes and its complications through various methods. Most of the studies reported the effects of oxidative stress on the body due to diabetes causing life-threatening complications. Oxidative stress is a condition where the production of free radicals exceeds the scavenging activity of the antioxidants (Birben et al., 2012). Although it is unclear how hyperglycaemia leads to increased oxidative stress, it is most probably due to the effects of increasing concentration of free radicals and the decreasing capacity of the cellular antioxidant defence system (Chung et al., 2003).

2.2 Aldose Reductase, Polyol Pathway and Its Inhibitors

Aldose reductase (AR) is mainly associated with diabetic complications. However, there are other diseases that are linked to AR such as inflammation and cancer (Sangshetti et al., 2014). Thus, the inhibition of AR is favourable in finding the cure for these diseases. AR has been reported to be isolated and purified from various animal and human tissues such as the eyes, liver, kidney and testis (Tang et al., 2012).

2.2.1 Polyol Pathway Mechanism and Oxidative Stress

Under normal blood glucose level in mammals, glucose is mainly phosphorylated into glucose-6-phosphate by hexokinase during glycolysis. Only about 3% of non-phosphorylated glucose enters the polyol pathway. However, with excess glucose, there will be influx of polyol pathway (Tang et al., 2012).

Polyol pathway consists of two enzymatic reactions. Firstly, AR will reduce glucose to sorbitol and this reaction will also convert nicotinamide adenine dinucleotide phosphate (NADPH) to NADP⁺ (oxidised form of NADPH). Then, sorbitol dehydrogenase (SDH) will oxidize sorbitol to fructose, thus producing nicotinamide adenine dinucleotide (NADH) from NAD⁺ (oxidised form of NADH) (Aslan & Beydemir, 2017; Tang et al., 2012). Figure 2.1 shows the reactions involve in polyol pathway.

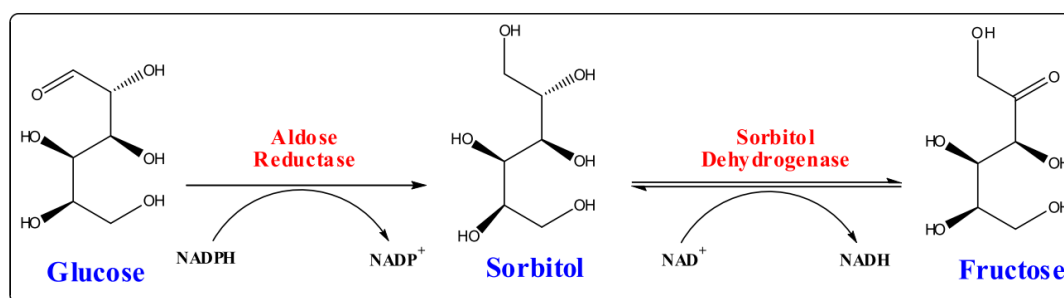


Figure 2.1 Polyol pathway (Aslan & Beydemir, 2017).

Since the conversion of glucose to sorbitol is the rate-determining step in this pathway (Ramana & Srivastava, 2010), sorbitol will be accumulated during hyperglycaemia. This results in osmotic imbalance since sorbitol is not readily diffuse through cell membrane and accumulates within the cells. The accumulation of sorbitol and fructose was reported as the cause of retinopathy in diabetic animals (Lorenzi, 2007).

This pathway also consumes NADPH cofactor that is needed by glutathione reductase, an enzyme which is responsible to produce reduced glutathione (GSH). GSH is an antioxidant and important scavenger of reactive oxidative species (ROS) (Giacco & Brownlee, 2010). The number of NADH cofactor will increase, leading to increasing oxidative stress since NADH is the substrate for NADH reductase which in turn produces additional ROS (Morré et al., 2000).

Fructose which is the end product of polyol pathway and its metabolites, fructose-3-phosphate and 3-deoxyglucosone, are more potent glycation agents than glucose. The influx of glucose through the polyol pathway would increase advance glycation end products (AGEs) formation which is known to cause oxidative stress (Chung et al., 2003). Figure 2.2 summarizes the possible metabolic pathways for glucose.

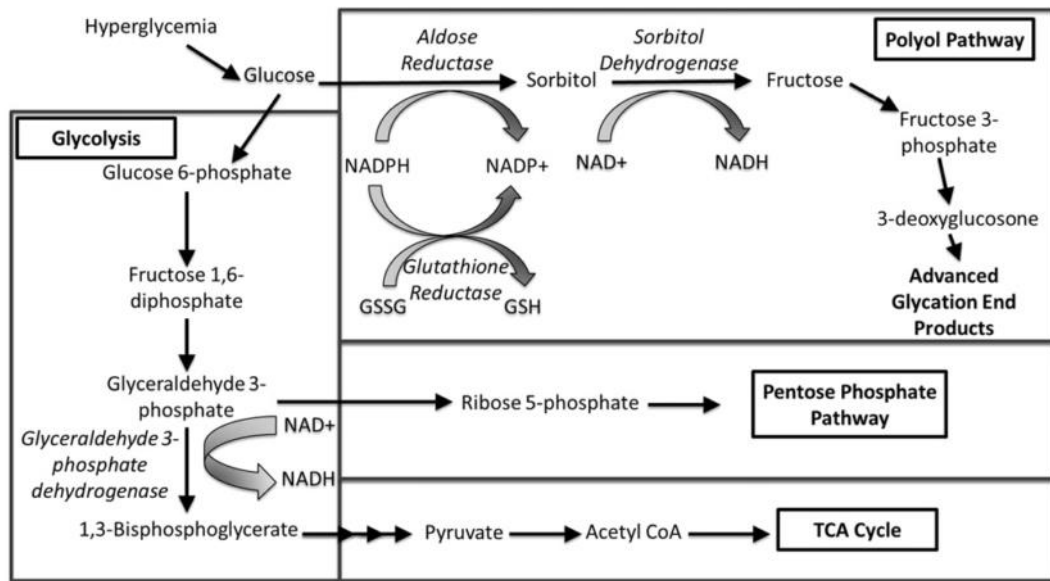


Figure 2.2 Possible pathways for glucose (Gallagher et al., 2016).

The mechanism of the aldehyde reduction in polyol pathway involves two steps. The first step is the transfer of hydride from the nicotinamide moiety of NADPH to the aldehyde's carbonyl carbon. The second step is the proton donation to reduce the carbonyl group to an alcohol. However, several main features remain unclear. It is unknown whether the reaction occurs in a concerted or stepwise manner and it is also not clear which of the proximal residues, Tyr48 or His110, acts as the proton donor (Dréanic et al., 2017; Nakano & Petrash, 1996).

2.2.2 Structure of Aldose Reductase

Aldose reductase (AR) was first identified by Hers (1956) as a protein with glucose reducing activity. AR belongs to the aldo-keto reductase super family and it is the first enzyme in the polyol pathway (Muthenna et al., 2009). It consists of a single polypeptide chain with 316 amino acids (Howard et al., 2004). The structure of AR folds into a $(\beta/\alpha)_8$ TIM-barrel with the active site located at the C-terminal region of the enzyme, as shown in Figure 2.3 (Steuber et al., 2007). The adjacent strands are connected by eight parallel α -helices running antiparallel to the β -sheets (El-Kabbani et al., 1998). Additionally, the NADPH cofactor binds to the bottom of the active site with the nicotinamide moiety pointing towards the active site. The crystal structure of AR coloured based on the secondary structure with NADP⁺ cofactor and bound ligand (IDD 594) is shown in Figure 2.3. Figure 2.4 shows the reduction of NADP⁺ (the oxidised form of NADPH) to NADPH.

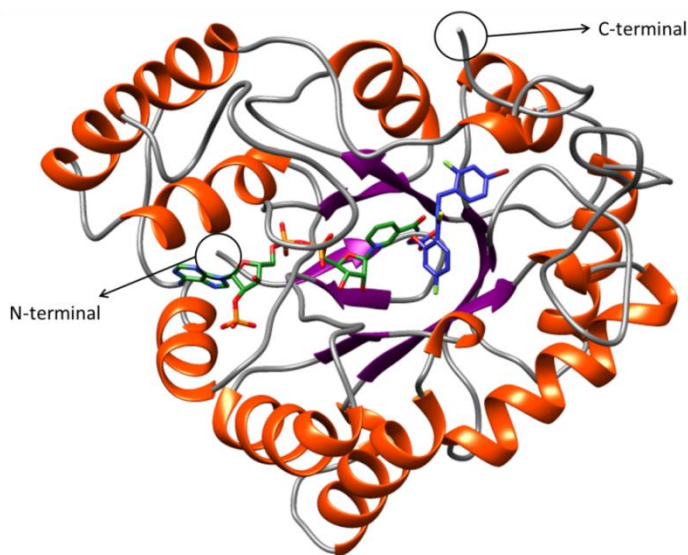


Figure 2.3 Crystal structure of aldose reductase with cofactor NADP⁺ (green) and the bound ligand IDD 594 (blue) from Protein Data Bank with PDB ID of 1US0 (Howard et al., 2004). The α -helices are highlighted in orange while the β -sheets are highlighted in purple colour. The coils are coloured in grey. The graphic is prepared using Chimera software.

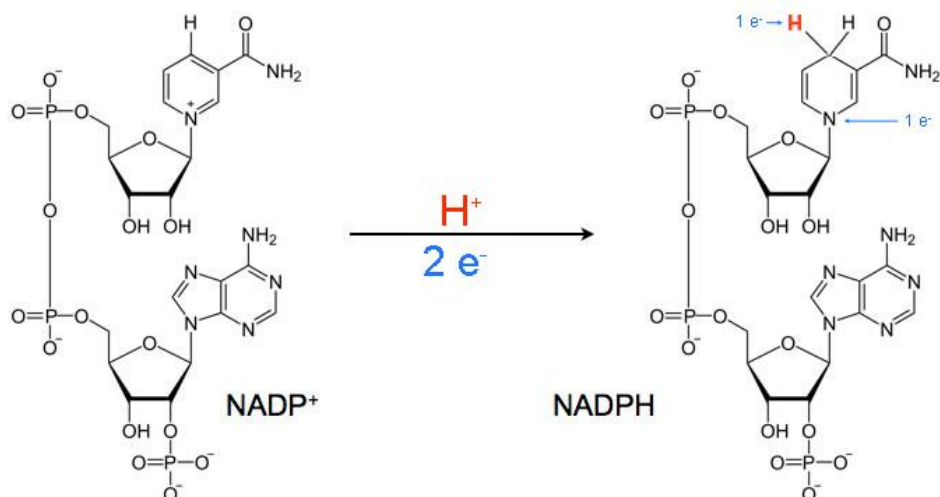


Figure 2.4 The reduction of NADP⁺ (the oxidised form of NADPH) to NADPH.

The binding site of AR is composed of a rigid anion binding pocket and a very flexible specificity pocket. The anion binding site is formed mostly by Tyr48, His110, Trp111 and the cofactor, NADP⁺ (Gopinath et al., 2016) meanwhile the specificity pocket consists of Ala299, Leu300 and Phe122 (Steuber et al., 2006). Figure 2.5 shows the binding pocket of AR based on their degree of flexibility. The specificity pocket can change its conformation to accommodate ligand of different sizes and shapes (Steuber et al., 2006). This leads to a broad range of structurally diverse ligands occupying the binding pocket. The hydrophobic specificity pocket can also present in two states; open and close, depending on the occupied ligand (Steuber et al., 2007). According to Gopinath et al. (2016), the Phe122 and Leu300 act as the gatekeepers that can seal or give access to the binding pocket, but the main flexibility is granted by the backbones of Ala299 and Leu300. This is confirmed by the different conformations of Leu300 side chains that can determine whether AR is in close or open state.

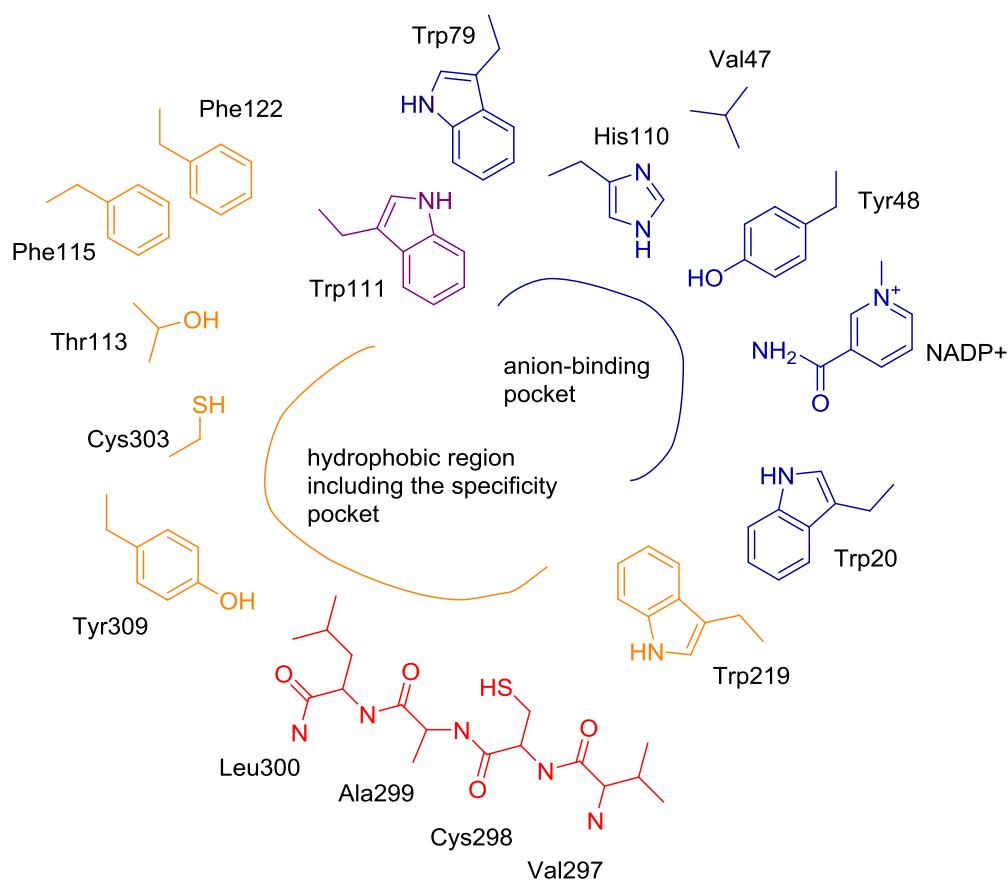


Figure 2.5 The binding pocket of AR in order of increasing degree of flexibility (blue < purple < orange < red) (Gopinath et al., 2016; Sotriffer et al., 2004).

2.2.3 Development of Aldose Reductase Inhibitors

Aldose reductase inhibitors (ARIs) have been widely investigated to prevent the increasing rate of polyol pathway in hyperglycaemic patient. Many aldose reductase inhibitors (ARIs) have been discovered but most of them have undesirable side effects (Pathania et al., 2013) such as high toxicity and less viability (Grewal et al., 2016). Only epalrestat (Figure 2.6) has passed the clinical trials and is marketed in Japan, China and India (Zhu, 2013). Fidarestat, another AR inhibitor candidate, is in phase III clinical trials and has been found to be safe (Ramunno et al., 2012). Although there are many classes of AR inhibitors (ARIs) (Grewal et al., 2016), the two most common classes of ARIs are spirohydantoin (e.g.: sorbinil) and carboxylic

acids (e.g.: tolrestat and epalrestat) (Rastelli et al., 2002). Due to the unwanted side effects such as renal and liver toxicity (Grewal et al., 2016), natural sources of ARIs with less toxicity and other harmful side effects were sought out by many researchers (Veeresham et al., 2014). Some of them are flavonoids (Patil & Gacche, 2017), alkaloids (Seo et al., 2016), phenolic acid (Alim et al., 2017) and polyphenols (Manivannan et al., 2015). The structures of well-known ARIs are shown in Figure 2.6.

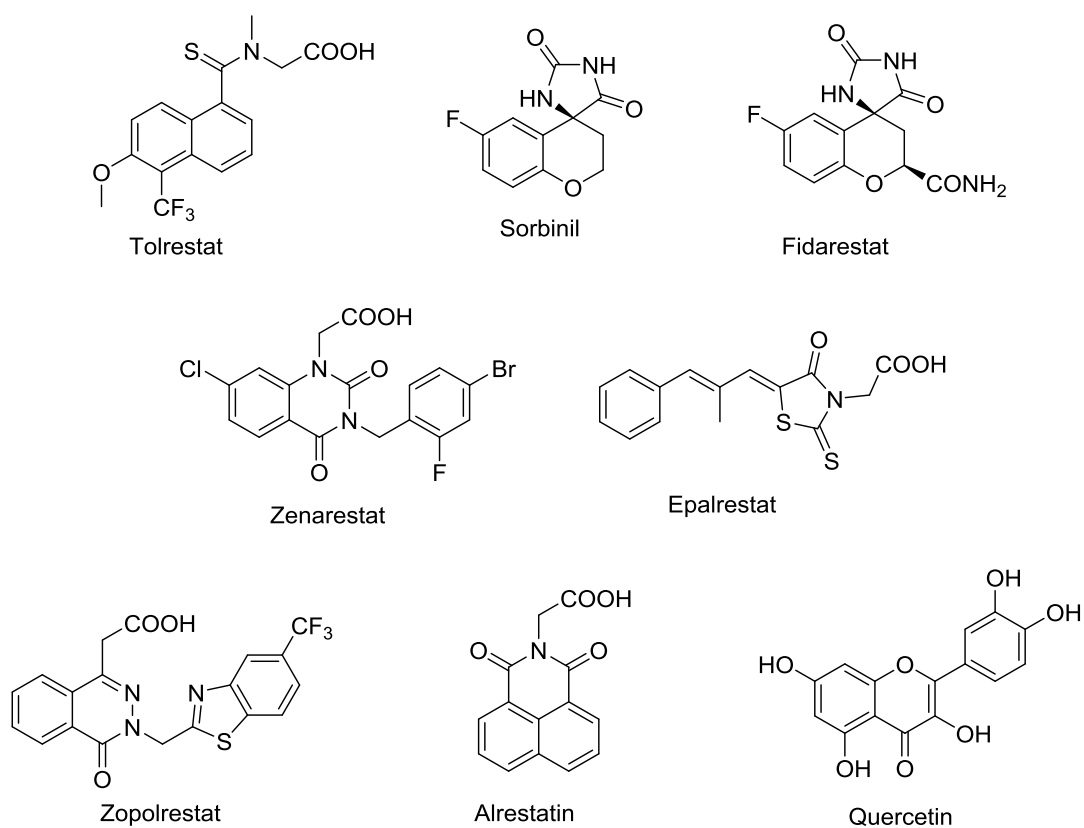


Figure 2.6 Chemical structures of known ARIs.

2.3 Flavonoids and Catechin

Flavonoids are a class of compounds with polyphenolic structures (Figure 2.7) mainly found in various parts of plants such as fruits, stems, leaves, barks and flowers. They are also found in several beverages such as tea, wine, and cocoa. Flavonoids can be categorised in several subgroups such as flavans, flavones, flavonols, and isoflavones (Panche et al., 2016). Figure 2.8 shows examples of different classes of flavonoids and their structures.

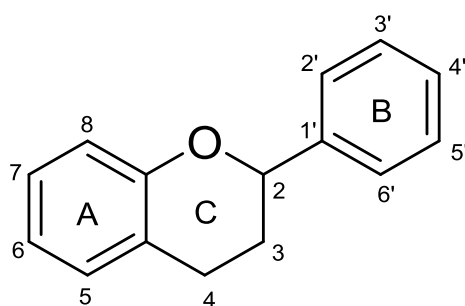


Figure 2.7 Basic structure of flavonoid.

Table 2.2 Classes of flavonoids and their examples.

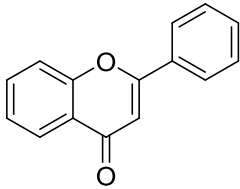
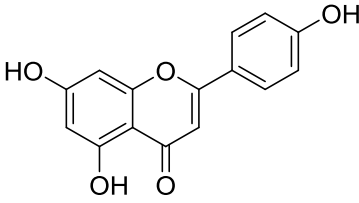
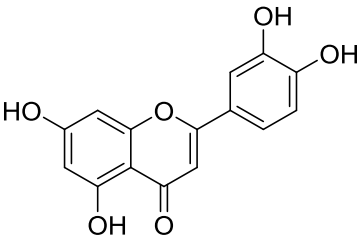
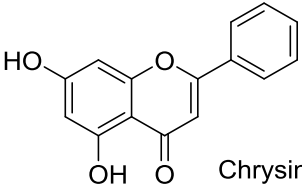
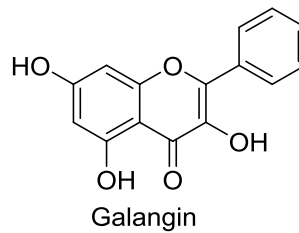
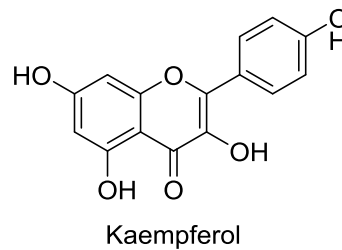
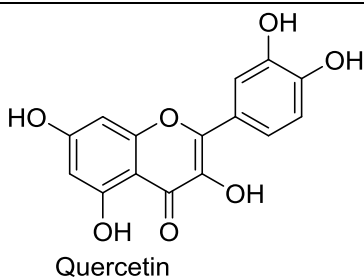
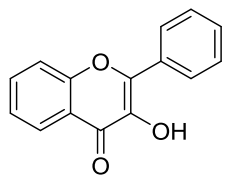
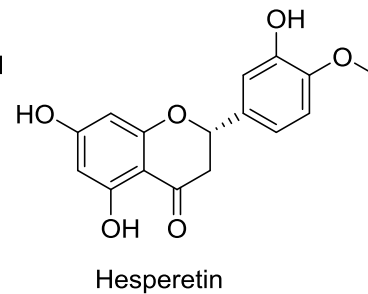
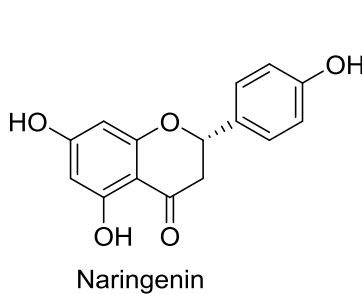
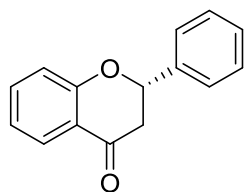
Classes of flavonoid	Examples
Flavones	  Apigenin  Luteolin  Chrysin

Table 2.2 Continued

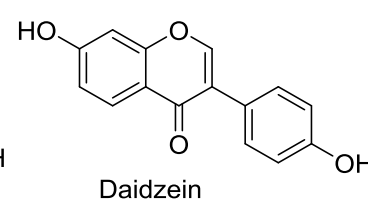
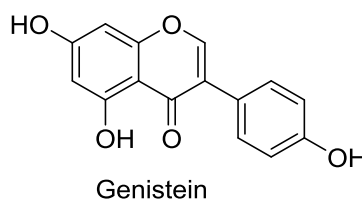
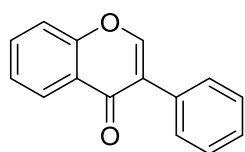
Flavonols



Flavonones



Isoflavones



Flavononol

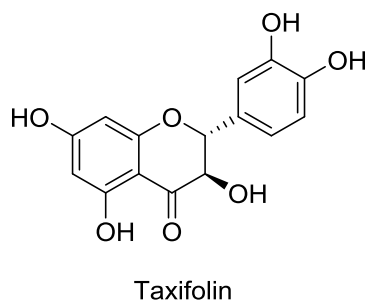
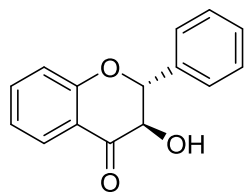
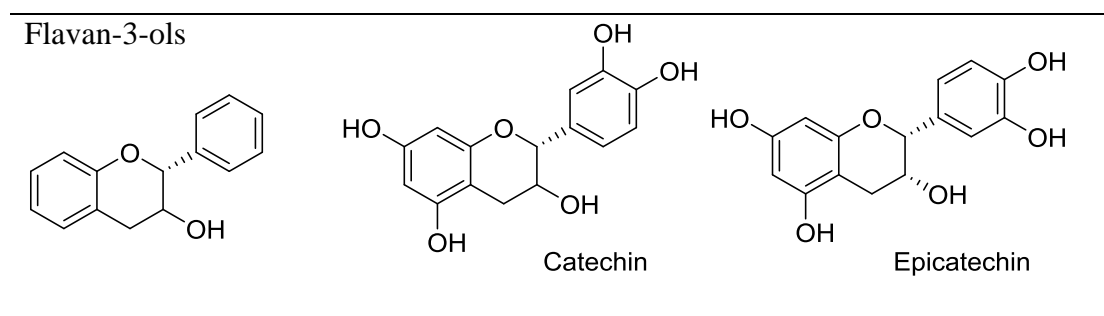


Table 2.2 Continued



Flavonoids have been reported to exhibit biological activities such as antioxidant (Hosseinzadeh et al., 2013), antibacterial (Xie et al., 2015), anti-inflammatory (Pan et al., 2010), anti-diabetic (Vinayagam & Xu, 2015), and anticancer (Chahar et al., 2011). Flavonoids are mainly known for its properties in scavenging free radicals and/or chelating metal ions (Kumar & Pandey, 2013). Flavonoids can interact with radicals which render them inactive due to the high reactivity of the hydroxyl group of the flavonoids, based on the Equation 2.1 below (Nijveldt et al., 2001):



The search for ARIs among flavonoids has been widely known and studied. For example, Bhadada et al. (2016) has studied the effect of *Tephrosia purpurea* plant extract in diabetic cataract. The extraction of the plant contains flavonoids with the presence of rutin and quercetin and it was tested on rats indicating successful delay in the development of cataract. The authors also conducted molecular docking study to investigate the interactions of AR with the flavonoids. There are also studies

on the commercially available flavonoids against AR (Madeswaran et al., 2012b; Madeswaran et al., 2013).

Matsuda et al. (2002) has summarized the structural requirement of flavonoids and other related compounds for AR inhibition activity. The results suggested the following structural requirements of flavonoid:

1. The flavones and flavonols having the 7-hydroxyl and/or catechol moiety at the B ring (the 3',4'-dihydroxyl moiety) display stronger activity;
2. The 5-hydroxyl moiety does not affect the activity;
3. The 3-hydroxyl and 7-O-glucosyl moieties reduce the activity;
4. The 2–3 double bond enhances the activity;
5. The flavones and flavonols having the catechol moiety at the B ring exhibit stronger activity than those having the pyrogallol moiety (the 3',4',5'-trihydroxyl moiety).

The authors also mentioned that catechins and isoflavones show less activity compared to flavones.

Catechin is a member in flavonoid family and within the flavan-3-ols subgroup (Table 2.2) that are found mainly in tea. Recently, Ganugapati and the co-workers (2017) have studied the interactions of flavonoids in green tea against AR activity at *in silico* level. Most of the flavonoids extracted were catechin derivatives. The results conclude that a few compounds in the extraction could be possible ARIs.

Murata et al. (1994) previously reported that green tea extract containing catechins were able to inhibit AR. The compounds identified to strongly inhibit AR were (-)-epicatechin, (-)-epicatechin gallate, and (-)-epigallocatechin gallate. The results also suggested that the catechol-type catechins inhibited AR better than

pyrogallol catechins which is in correlation with the results from Matsuda et al. (2002).

2.4 Molecular Modelling

Molecular modelling has been used extensively over the years and is a powerful tool used in drug design. Molecular modelling involves the construction and manipulation of three-dimensional structures of molecules and physical chemistry. It is also referred to as computational chemistry as it includes a range of computerized technique based on theoretical chemistry and experimental data to predict the molecular and biological properties of molecules (Nadendla, 2004). Potent inhibitors for aldose reductase have been widely searched using computational methods. This results in a vast number of x-ray crystallography structures of AR in Protein Data Bank (PDB, Berman et al., 2000); total up to 145 structures for human and animal as of February 2018.

2.4.1 Molecular Docking

Molecular docking is a method which predicts the preferred binding orientation of one molecule to another molecule to form a stable complex. Docking plays a major role in drug design as it is often used to predict the binding orientation of small molecules (drug candidate) to their target protein and hence predict the affinity and the activity of the small molecules (Mukesh & Rakesh, 2011). Figure 2.8 shows the schematic illustration of protein-ligand molecular docking.

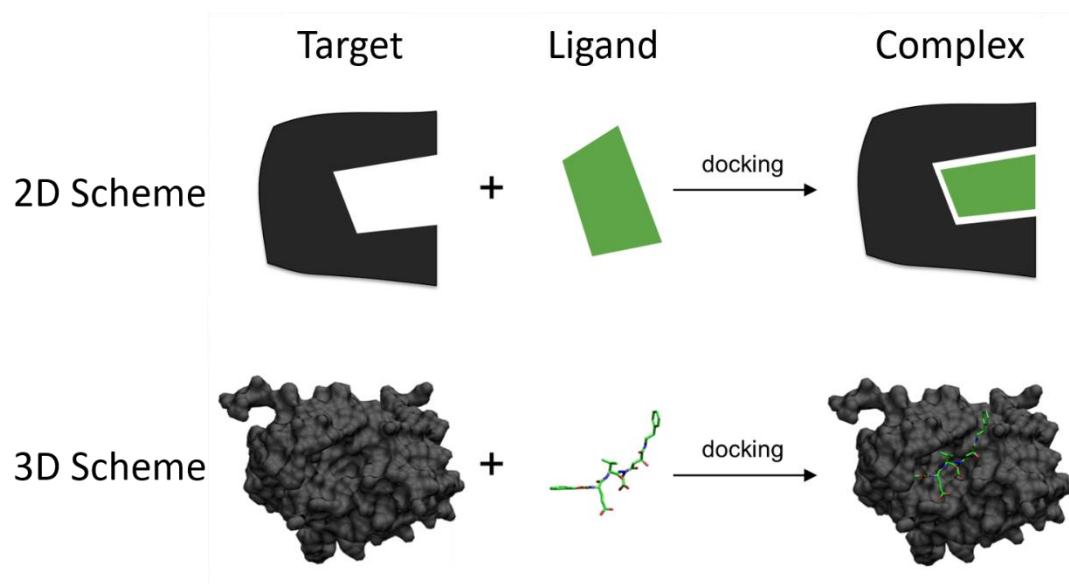


Figure 2.8 Schematic illustration of docking a small molecule or ligand (green) to a protein or macromolecule (black) to produce a stable protein/ligand complex.

Over the last 20 years, more than 60 different docking tools and programs has been developed for academic and commercial use (Pagadala et al., 2017). Examples of docking softwares are FlexX (Rarey et al., 1996), GOLD (Jones et al., 1997), Autodock Vina (Trott & Olson, 2010), GLIDE (Friesner et al., 2004), ICM (Abagyan et al., 1994), DOCK (Kuntz et al., 1982) and AutoDock (Morris et al., 2009).

Due to the flexibility of aldose reductase, a diverse class of inhibitors has been found with different structures and functional groups. Table 2.3 summarizes the findings of these AR inhibitors via molecular docking over the last 10 years. Based on the Table 2.3, it can be concluded that the most popular software used for docking of AR and inhibitor candidates was AutoDock program.

Table 2.3 Summary of the studies reported on ARIs via molecular docking and molecular dynamics simulation methods used (if any) over the last 10 years.

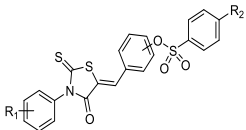
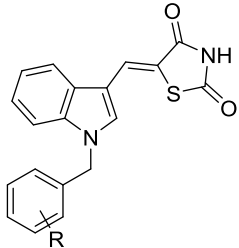
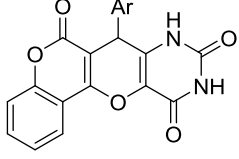
PDB ID of AR used (Resolution)	Ligands used for docking	Docking software	MD (software, force field, solvent and others)	References
3FX4 (1.99 Å) and 1US0 (0.66 Å)	Thioxothiazolidin one-sulfonate conjugates 	MOE-Dock module	-	Andleeb et al., 2017
1US0	Thiazolidine-2, 4-dione analogues 	CDOCKER module in Discovery Studio 4.1.	Desmond software, OPLS 2005 force field, and MM-GBSA analysis	Chadha & Silakari, 2017
3G5E (1.80 Å)	21 compounds from green tea extracts	Autodock 4.0	-	Ganugapati et al., 2017
2DUX (1.60 Å)	10 chromeno-pyrano pyrimidine compounds 	Autodock 4.0	-	Hese et al., 2017
1AH0 (2.30 Å)	20 flavanone derivatives and quercetin as standard	Biopredicta module in Vlife MDS 4.3	-	Kondhare et al., 2017

Table 2.3 Continued

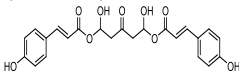
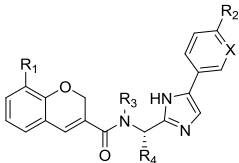
1PWM (0.92 Å)	1,5-di-hydroxy- 1,5-di-[(E)-3-(4- hydroxyphenyl)- 2-propenoic]-3- pentanonyl ester (DHDP)	Surlex-dock software	-	Wang et al., 2017
				
1US0	Rutin, quercetin, fidarestat, lupeol, tephrosin, degurelin, rotenone, and elliptone	Surflex- dock module of SYBYL	-	Bhadada et al., 2016
1Z3N (1.04 Å) and 1US0	2H-chromene-N- imidazolo-amino acid conjugates	Glide standard precision dock application by Schrodinger	-	Gopinath et al., 2016
				
2DUX	Monohydroxylate d flavonoids	Autodock 4.2	-	Patil et al., 2016
1US0 (chosen after cross- docking analysis), 1PWM, 1Z8A (0.95 Å), 2PZN (1.00 Å), 3U2C (1.00 Å), 1Z3N, and 1T41 (1.05 Å)	5 flavonoids were picked out from 54 studied flavonoids.	Glide extra precision program.	-	Vyas et al., 2016

Table 2.3 Continued

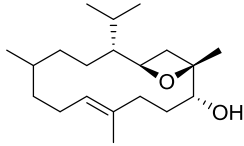
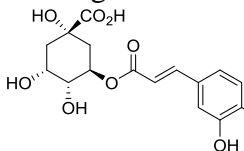
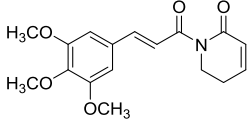
4CGA (0.90 Å), 4LAU (0.84 Å), and 1US0	Gingerenone A, gingerenone B, quercetin, lariciresinol, calebin A, gingerenone C, ranirestat, epalrestat, and sorbiniol	Schrodinger Glide (standard precision then extra precision).	Desmond software, OPLS 2005 force field, orthorhom bic box, SPC water models and MM- GBSA analysis	Antony & Vijayan, 2015
2FZD (1.08 Å)	Polyphenols: Acacetin, ferulic acid, protocateuic acid, gallic acid, cinnamic acid, vanillic acid, and syringic acid	Autodock 4.2.	Gromacs 4.5.4, Amber03 force field	Manivann an et al., 2015
Not stated	Quercetin, naringin, tolrestat, and fidorestat	Cdocker, Ligand Fit, and Libdock	-	Rajasuloc hana & Sujith, 2015
2FZD	Epalrestat analogues	FlexX software.	-	Reddy et al., 2014
2NVC (1.65 Å)	Incensole and co- crystalized ligand 	MOE package.	-	Zaki, 2014
1US0, 2FZD, 2IKG (1.43Å), 2INE (1.90 Å), and 3G5E	Chlorogenic acid 	Molgro Virtual Docker (MVD) Software	-	Naeem et al., 2013

Table 2.3 Continued

1US0	Compounds from <i>Rauvolfia serpentine</i> extract	Autodock Vina 1.1.2.	Gromacs 4.0.7, Gromos96 4a1 force field, cubic box and SPC water models	Pathania et al., 2013
2PDK (1.55 Å), 1US0, and 2FZD	Ligands obtained from virtual screening	The FlexX module in Sybyl 7.3	Amber 11 package, AMBER ff99SB force field, octahedral box and TIP3P water model	Wang et al., 2013
1PWM	Compounds from <i>Gentiana lutea</i> extracts	Discovery 2.7 package	-	Akileshwari et al., 2012
1EL3 (1.70 Å)	Apigenin, baicalin, daidzein, epigallocatechin, galangin, genistein, hesperitin, naringenin, scopoletin, and epalrestat	Autodock 4.2	-	Madeswaran et al., 2012b
1AH3 (2.30 Å)	Virtual screening of 267 compounds	GOLD, Patchdock, eHITS, Molegro, MEdock, Autodock Vina	-	Muppalaneni & Rao, 2012

Table 2.3 Continued

1PWM	Piplartine derivatives and fidarestat 	Discovery 2.7 package and GOLD software	-	Rao et al., 2012
3DN5 (1.45 Å)	9 ligands used for docking after pharmacophore modelling	LigandFit protocol in Discovery Studio	Gromacs 4.0.5, Gromos96 force field, cubic box	Sakkiah et al., 2012
3RX3 (1.90 Å)	Farobin, gericudranin, glaziovianin, rutin, xanthotoxin, and epalrestat	Autodock 4.2	-	Umamahe swari et al., 2012
1Z3N	Indole acetic acid derivatives	Autodock 4.2.	-	Juskova et al., 2011
1PWM	Rutin and quercetin	Discovery 2.7 package	-	Reddy et al., 2011
1AH0	6 flavone derivatives	Fast Rigid Exhaustive Docking (FRED) version 2.1	-	Sekhar et al., 2011
1US0	Series of pyrrole based chemotypes (seven compounds)	GLUE program in the GRID package	-	Pegklidou et al., 2010
2PDK, 1US0, 2FZD	Virtual screening of 12 structures	Autodock 4.0	-	Cosconati et al., 2009
2A00 – replaced with 3H4G (1.85 Å) and 1PWM	Curcumin	FlexX module in SYBYL 7.0 (Tripos)	-	Muthenna et al., 2009